AMERICAN SOCIETY FOR MICROBIOLOGY | mSphere®

RESEARCH ARTICLE

Heterogeneity and Recombination of Foot-and-Mouth Disease Virus during Multi-Strain Coinfection of Cattle

Carolina Stenfeldt,[a,b] Ian Fish,[a,b] Haillie C. Meek,[a,c] Jonathan Arzt[a]

[a]Foreign Animal Disease Research Unit, Agricultural Research Service, United States Department of Agriculture, Plum Island Animal Disease Research Center, Greenport, New York, USA

[b]Department of Diagnostic Medicine/Pathobiology, College of Veterinary Medicine, Kansas State University, Manhattan, Kansas, USA

[c]PIADC Research Participation Program, Oak Ridge Institute for Science and Education, Oak Ridge, Tennessee, USA

ABSTRACT Superinfection of cattle persistently infected with foot-and-mouth disease virus (FMDV), with a heterologous FMDV strain has been shown to generate novel recombinant viruses. In this study, we investigated the pathogenesis events within specific tissues associated with FMDV coinfections in cattle subjected to either simultaneous or serial exposure to two distinct strains of FMDV. Both strains of FMDV (one each of serotypes O and A) were similarly localized to the nasopharyngeal mucosa during the early stages of infection. However, while no recombinant FMDV genomes were recovered from simultaneously coinfected cattle, interserotypic recombinants were isolated from nasopharyngeal tissue samples obtained at 48 h after heterologous superinfection of a persistently infected FMDV carrier. Additionally, analysis of FMDV genomes obtained from replicate nasopharyngeal tissue samples demonstrated that adjacent segments of the mucosa were sometimes infected by distinct viruses, demonstrating a multifocal and heterogeneous distribution of FMDV infection during primary and persistent phases of infection. This work indicates that superinfection of FMDV carriers may be an important source of emergent recombinant strains of FMDV in areas where multiple strains are cocirculating.

IMPORTANCE Foot-and-mouth disease (FMD) is a socioeconomically impactful livestock disease with a complex epidemiology and ecology. Although recombinant viruses have been identified in field samples, the mechanisms of emergence of those viruses have never been elucidated. This current study demonstrates how serial infection of cattle with two distinct serotypes of FMD virus (FMDV) leads to rapid generation of recombinant viruses in the upper respiratory tracts of infected animals. This finding is particularly relevant in relation to the management of persistently infected FMDV carrier cattle that can maintain subclinical FMDV infection for months to years after an initial infection. Such carrier animals may function as mixing vessels that facilitate the emergence of novel recombinant FMDV strains in areas where multiple virus strains are in circulation.

KEYWORDS FMD, FMDV, foot-and-mouth disease, cattle, foot-and-mouth disease virus, infectious disease, pathogenesis, recombination

Foot-and-mouth disease (FMD) is a high-consequence viral infection of cloven-hoofed livestock caused by foot-and-mouth disease virus (FMDV; genus *Aphthovirus*, family *Picornaviridae*) (1). The global distribution of FMD, which is endemic in substantial parts of Africa and Asia, has a critical impact on the regulation of international trade in animals and animal products (2, 3). Therefore, considerable financial resources are invested in FMD control, both by countries directly affected by the consequences of the disease itself as well as by those wanting to prevent FMDV incursions (4, 5).

The molecular epidemiology of FMDV is complicated because there are seven distinct serotypes, with multiple lineages and subtypes within those serotypes (6). No

Editor Angela L. Rasmussen, University of Saskatchewan

Address correspondence to Jonathan Arzt, Jonathan.Arzt@USDA.GOV, or Carolina Stenfeldt, Carolina.Stenfeldt@USDA.GOV.

The authors declare no conflict of interest.

Received 12 December 2022
Accepted 29 March 2023
Published 24 April 2023

protection across serotypes is conferred by vaccination or previous infection (7). Additionally, vaccination does not protect against subclinical infection of the upper respiratory tract in exposed bovines (8–11).

Studies of FMDV phylogenetics based on whole-genome sequencing of field viruses have shown that recombination involving different FMDV serotypes is common (12–14). However, until recent years, most phylogenetic studies of FMDV have been based exclusively on VP1 sequencing, which fails to capture the complexities of viral recombination occurring in nonstructural coding regions.

A substantial proportion of ruminants that recover from either clinical or subclinical neoteric (primary) FMDV infection will progress to a persistent subclinical phase of FMDV infection that may last for several months to years (15). In cattle, both primary and persistent FMDV infection has been localized to distinct regions within the nasopharyngeal mucosa (8, 9, 16, 17). In contrast, persistent FMDV infection in African buffalo (*Syncerus caffer*), an important natural reservoir host for the virus, has been demonstrated to occur in epithelial crypts of the palatine tonsils (18, 19).

The epidemiological relevance of FMDV carriers is controversial. A historical disparity exists between findings supporting infectiousness and counterclaims of irrelevance. The potential for contagion is suggested by the well-established fact that infectious virus is present in the upper respiratory tract of carriers, and it has further been shown that deposition of unadulterated oropharyngeal fluid (OPF) derived from persistently infected cattle into the upper respiratory tracts of naive recipient cattle will cause fulminant disease (10, 20). Conversely, several small-scale experimental studies have failed to demonstrate transmission of FMDV from persistently infected cattle to naive animals kept in close contact for longer durations (21–23). Based on current regulations dictated by the World Organization for Animal Health, the presence of FMDV carriers is not tolerated in any country seeking to achieve FMD-free status (24). Additionally, due to the risk of subclinical infection in vaccinated animals, the waiting period required to regain official FMD-free status following an outbreak is substantially increased if vaccination is used as part of disease control efforts (24, 25).

We have previously demonstrated that heterologous superinfection of persistently infected FMDV carrier cattle led to detection of dominant interserotypic recombinant genomes in oropharyngeal fluid samples in 5 of 12 study animals as early as 10 days after superinfection. In contrast, no viral recombinants were detected in samples from animals that were simultaneously coinfected with the same two viruses (26). These findings indicate that under experimental conditions, persistently infected FMDV carrier cattle function as mixing vessels. In areas where multiple variants of FMDV are in circulation, this mechanism may facilitate the emergence of novel recombinant viral strains.

The current investigation is based on analysis of antemortem and tissue samples from cattle that were euthanized at early time points following simultaneous coinfection or heterologous superinfection. Through a combined approach using molecular diagnostic techniques, immunohistochemistry, and next-generation sequencing, we explored the early pathogenesis of FMDV coinfection and demonstrate that interserotypic recombinants can be isolated from nasopharyngeal tissue samples within 48 h of heterologous superinfection. Our findings affirm the relevance of persistently infected FMDV carrier cattle as likely sources of recombinant FMDV strains and reiterate that superinfected FMDV carriers represent a distinct category of animals that have not previously been examined for their epidemiological relevance.

RESULTS

Three groups of four cattle each were infected with FMDV A24 Cruzeiro (FMDV A24) and FMDV O1 Manisa (FMDV O1M) simultaneously (Group 1) or separated by 21 (Group 2) or 35 days (Group 3) (Fig. 1). Two animals from each group were euthanized for postmortem tissue harvest at 24 and 48 h after the simultaneous (Group 1) or final

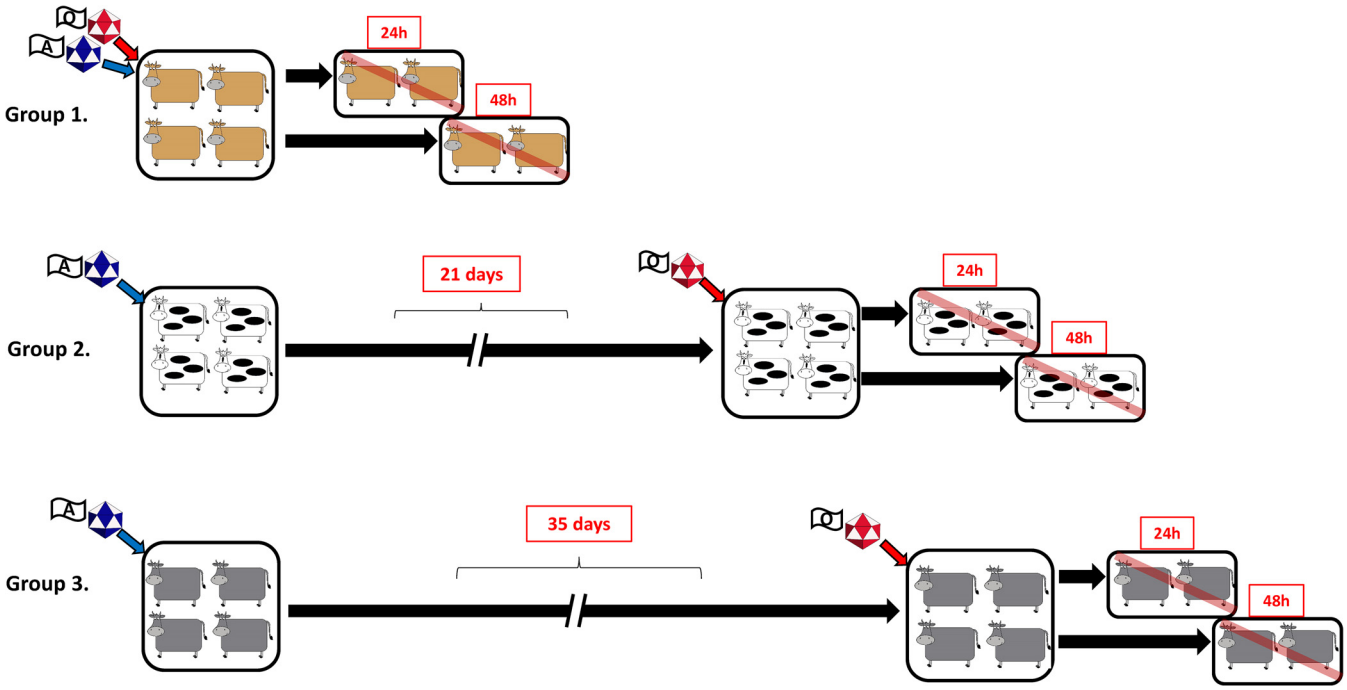

FIG 1 Study design. The study comprised three groups of four cattle each. Group 1 were simultaneously infected with foot-and-mouth disease virus (FMDV) O1 Manisa and A24 Cruzeiro on day 0, Group 2 were infected with FMDV A24 Cruzeiro on day 0 and superinfected with FMDV O1 Manisa on day 21, and Group 3 were infected with FMDV A24 Cruzeiro on day 0 and superinfected with FMDV O1 Manisa on day 35. Two animals from each group were euthanized for postmortem tissue harvest at 24 and 48 h after the final (or, for group 1, simultaneous) virus exposure.

(Groups 2 and 3) virus exposure. Additional animals within each cohort were monitored for longer durations (26).

Simultaneous coinfection. (i) Antemortem infection dynamics. The four animals in Group 1 were infected with a mixed inoculum containing equal quantities (10^6 $TCID_{50}$ [50% tissue culture infective dose]) of FMDV A24 and FMDV O1M. Nasal swabs were positive for both viruses by quantitative real-time reverse transcriptase PCR (qRT-PCR) in all four animals at 24 h postinfection (hpi) and at 48 hpi in one of the two animals kept to that time point, whereas the nasal swabs from the second animal were negative (Fig. 2). No viral RNA was detected in serum samples from the two animals euthanized at 24 hpi, whereas RNA from both viruses was detected in serum samples collected at 48 hpi in the two animals that were kept to that time point. Additionally, one serum sample obtained at 24 hpi from one of the animals kept through 48 h (ID no. 19-03) was positive for FMDV O1M RNA (Fig. 2). No clinical signs of FMD were observed in any of the animals in this group prior to euthanasia.

(ii) Tissue distribution of FMDV. FMDV tissue distribution was determined by strain-specific qRT-PCR systems, combined with virus isolation (VI) and confirmation of virus strain identities in VI supernatants by qRT-PCR. At 24 hpi, all nasopharyngeal tissue samples, comprised by the rostral and caudal segments of the dorsal surface of the soft palate and the dorsal nasopharynx, were positive for both viruses by qRT-PCR and VI (Fig. 3). Low quantities of FMDV A24 RNA, without concurrent isolation of infectious virus, were detected in the lingual and palatine tonsils from one animal each. Additionally, both viruses were isolated, with no FMDV RNA detected in the raw tissue samples, from the nasopharyngeal tonsils as well as from either the medial retropharyngeal or submandibular lymph nodes of both animals.

At 48 hpi, the distribution of FMDV in tissues was more widespread, consistent with concurrent detection of viremia of both viruses (Fig. 3). In addition to the nasopharyngeal mucosal samples, infectious virus was also detected in samples of the lungs as well as the lingual and palatine tonsils. Interestingly, infectious virus was also isolated

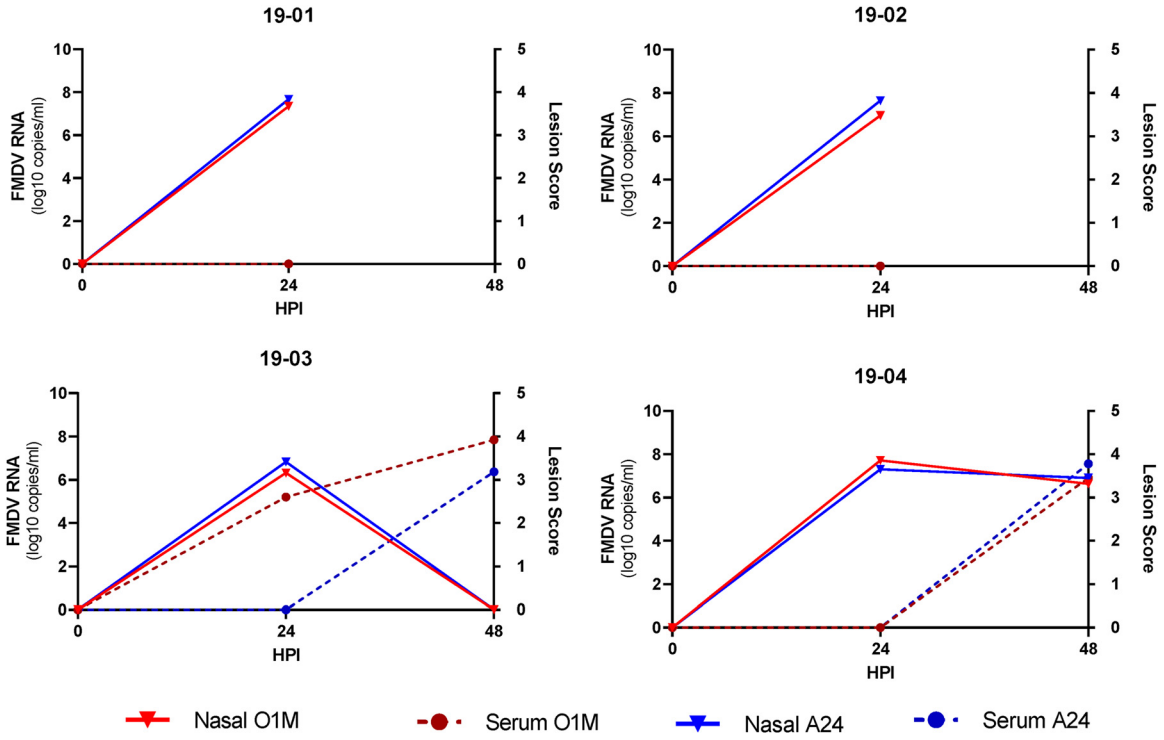

FIG 2 FMDV infection dynamics in simultaneously coinfected cattle. Strain-specific detection of FMDV RNA in nasal swabs (solid lines, triangular markers) and sera (hatched lines, circular markers) from cattle simultaneously infected with FMDV O1 Manisa (red) and FMDV A24 Cruzeiro (blue). Animals no. 19-01 and 19-02 (top row) were euthanized for tissue harvest at 1 day postinfection (dpi) and animals no. 19-03 and 19-04 (bottom row) were euthanized at 2 dpi. No FMD lesions were observed in any of the animals.

from lesion predilection sites, including the tongues of both animals and the coronary band and interdigital cleft skin of one animal, despite a lack of any grossly visible lesions at those sites (Fig. 3). Infectious virus was also, as at the earlier time point, isolated from select lymph nodes even though viral RNA quantities were too low to be detected in the original tissue macerates.

Overall, the distributions of the two viruses were similar and consistent with the distribution expected in animals infected with just one strain of FMDV.

Heterologous superinfection of FMDV carriers. (iii) Antemortem infection dynamics. Heterologous superinfection was investigated in two experimental groups: Group 2 was infected with FMDV A24 on day 0 and superinfected with FMDV O1M on day 21, whereas Group 3 was infected with FMDV A24 on day 0 and superinfected with FMDV O1M on day 35.

All animals were confirmed to have been infected by the first (FMDV A24) virus exposure with associated clinical FMD of expected severity observed in all but one individual (Fig. 4 and 5). FMDV A24 RNA was consistently detected in nasal swabs through 8 to 14 days, and in sera from 7 of the 8 animals through 6 to 8 days. One animal in Group 3 (ID no. 19-33) did not develop clinical FMD or viremia following inoculation, but infection was confirmed based on consistent detection of FMDV RNA in nasal swabs through 10 days postinfection (dpi) and detection of FMDV RNA as well of isolation of infectious virus from oropharyngeal fluid samples collected from 14 to 31 dpi (Fig. 5).

Seven of the eight animals were presumed to have been persistently infected with FMDV A24 at the time of superinfection with FMDV O1M, based on isolation of FMDV A24 from OPF samples up until 4 days prior to superinfection (Fig. 4 and 5). After this time point, OPF harvesting was paused to avoid potential interference with the pathogenesis of primary infection due to the scraping of the mucosal surface that is associated with collection of probang samples.

	24 HPI				48 HPI			
Animal ID	19-01		19-02		19-03		19-04	
Virus strain	A24	O1M	A24	O1M	A24	O1M	A24	O1M
Serum	-	-	-	-	3.36	4.85	4.56	3.90
Tongue		+			2.43	5.46	2.68	
Lingual tonsil	2.02				2.86	4.03	4.78	4.25
Palatine tonsil	+		3.75		+	+	3.06	+
Ventral soft palate					2.33	3.67	4.27	4.40
Dorsal soft palate - rostral	3.05	4.26	3.77	4.86	4.96	6.00	6.15	6.31
Dorsal soft palate - caudal	3.74	3.96	4.63	5.08	5.82	5.47	5.18	4.40
Nasopharyngeal tonsil	+	+	+	+	+	+	2.41	+
Dorsal nasopharynx - rostral	5.55	5.15	5.42	5.13	2.90	4.41	4.31	4.25
Dorsal nasopharynx - caudal	5.81	5.65	5.40	5.53	4.74	5.47	4.50	4.45
Lung - distal cranial lobe					2.92	+	2.64	
Lung - distal middle lobe					2.03	3.57	2.51	+
Interdigital cleft							2.92	
Coronary band							4.18	4.28
Medial retropharyngeal LN	+		+	+	+	+	+	+
Submandibular LN		+				+	1.95	
Popliteal LN					+	+	+	

FIG 3 FMDV distribution in bovine tissues following simultaneous coinfection. Strain-specific FMDV detection in tissue samples obtained at 24 and 48 h post-intranasopharyngeal deposition of a mixed inoculum containing equal quantities of FMDV O1 Manisa (red) and FMDV A24 Cruzeiro (blue). Numbers in table represent $\log_{10}$ genome copy numbers (GCN)/mg of FMDV RNA in tissue or $\log_{10}$ GCN/μL serum, for the specific virus. Color gradient indicates increasing FMDV RNA quantities in samples that were positive by both strain-specific real-time reverse transcriptase PCR (qRT-PCR) and virus isolation (VI), with virus specificity in VI supernatants determined by strain-specific qRT-PCR. Numbers in uncolored cells indicate quantities of FMDV RNA detected in samples that were negative by virus isolation for that specific virus; plus sign (+) indicates that virus isolation was positive but FMDV RNA content was below the limit of detection.

Animals in Group 2 were superinfected with FMDV O1M at 21 dpi. FMDV O1M RNA was detected in nasal swabs at 24 hpi in one of the two animals that were euthanized at that time point. Of the two animals that were euthanized at 48 hpi, FMDV O1M was detected in serum at 24 and 48 hpi in one animal. Shedding in nasal swabs was detected at 48 hpi in one animal and at both 24 hpi and 48 hpi in the other animal (Fig. 4). There was no clinical FMD observed in any animal after the superinfection within the period of observation.

In study group 3, which were superinfected at 35 dpi, FMDV O1M RNA was detected in nasal swabs of all four animals at 24 hpi (Fig. 5). Of the two animals euthanized at 48 hpi, one had FMDV O1M-positive nasal swabs at both 24 and 48 hpi and a positive serum sample at 48 hpi, whereas the other animal had a positive nasal swab at 24 hpi but negative samples at 48 hpi (Fig. 5). There were no signs of clinical FMD in any of the four animals after superinfection within the study period.

Tissue distribution of FMDV. (i) Superinfection on 21 dpi. The four animals in group 2 were presumed to be persistently infected with FMDV A24 at the time of superinfection based on isolation of FMDV A24 from OPF samples obtained at 14 and 17 dpi. This was confirmed in three of the animals by isolation of infectious FMDV A24 from nasopharyngeal tissue samples obtained at necropsies performed 22 and 23 days after FMDV A24 infection (corresponding to 24 and 48 h after superinfection with FMDV O1M; Fig. 6). FMDV A24 RNA was detected in a wider range of tissues compared to infectious virus, which is consistent with previous studies investigating tissue distribution of FMDV in convalescent animals (9, 16).

At 24 hpi, FMDV O1M was primarily isolated from nasopharyngeal tissues, with an additional VI-positive/qRT-PCR-negative sample from the palatine tonsil of one animal. As in Group 1, there was a wider distribution of infectious virus at 48 h after infection, specifically in the one animal from which FMDV O1M was also detected in serum (ID

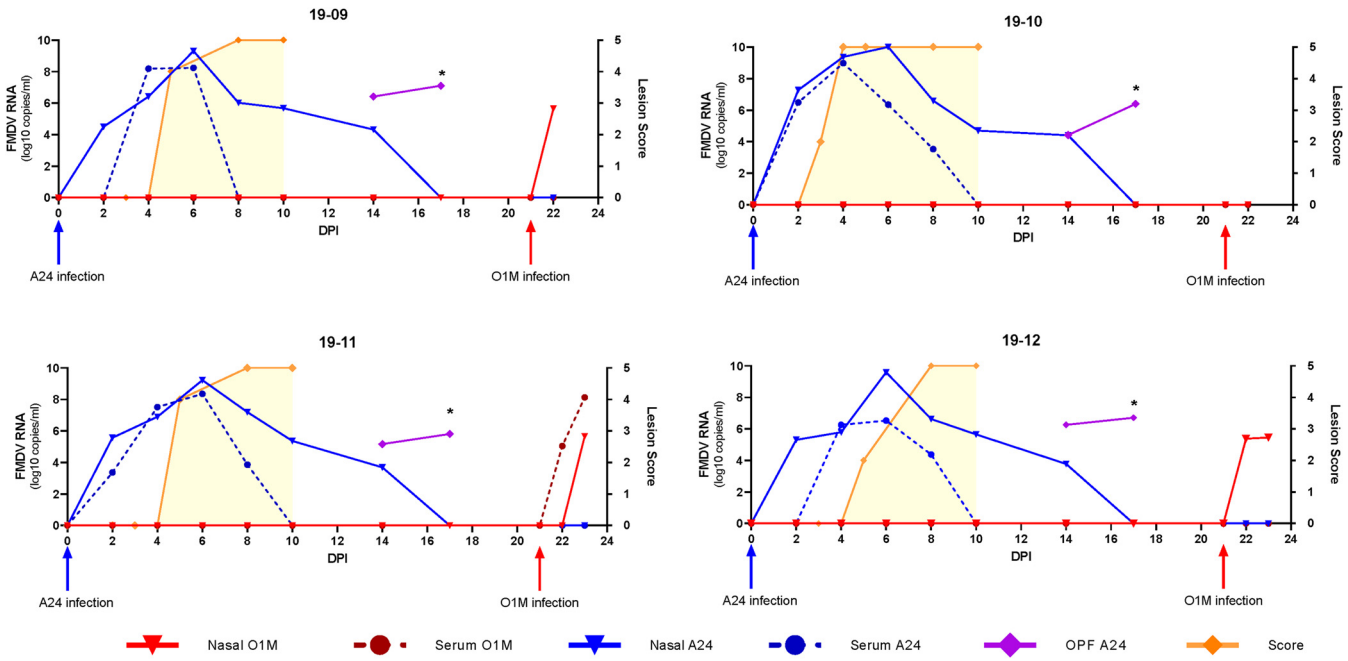

FIG 4 FMDV infection dynamics in cattle that were infected with FMDV A24 Cruzeiro on day 0 and superinfected with FMDV O1 Manisa on day 21. Strain-specific detection of FMDV RNA in nasal swabs (solid lines, triangular markers), sera (hatched lines, circular markers), and oropharyngeal fluid (OPF; purple line, diamond markers) from cattle sequentially infected with FMDV A24 Cruzeiro (blue and purple) and FMDV O1 Manisa (red). Shaded yellow area represents the cumulative lesion score observed through the first 10 days of infection. Animals no. 19-09 and 19-10 (top row) were euthanized for tissue harvest at 1 day post-superinfection, and animals no. 19-11 and 19-12 (bottom row) were euthanized at 2 days post-superinfection. Asterisk (*) indicates that OPF samples were only collected on days 14 and 17.

no. 19-11; Fig. 6). In this animal, FMDV O1M was isolated from samples of the lungs and lesion predilection sites (tongue and coronary band/interdigital cleft skin). However, in all animals, the highest quantities of FMDV RNA were found in the naso-pharyngeal mucosal samples.

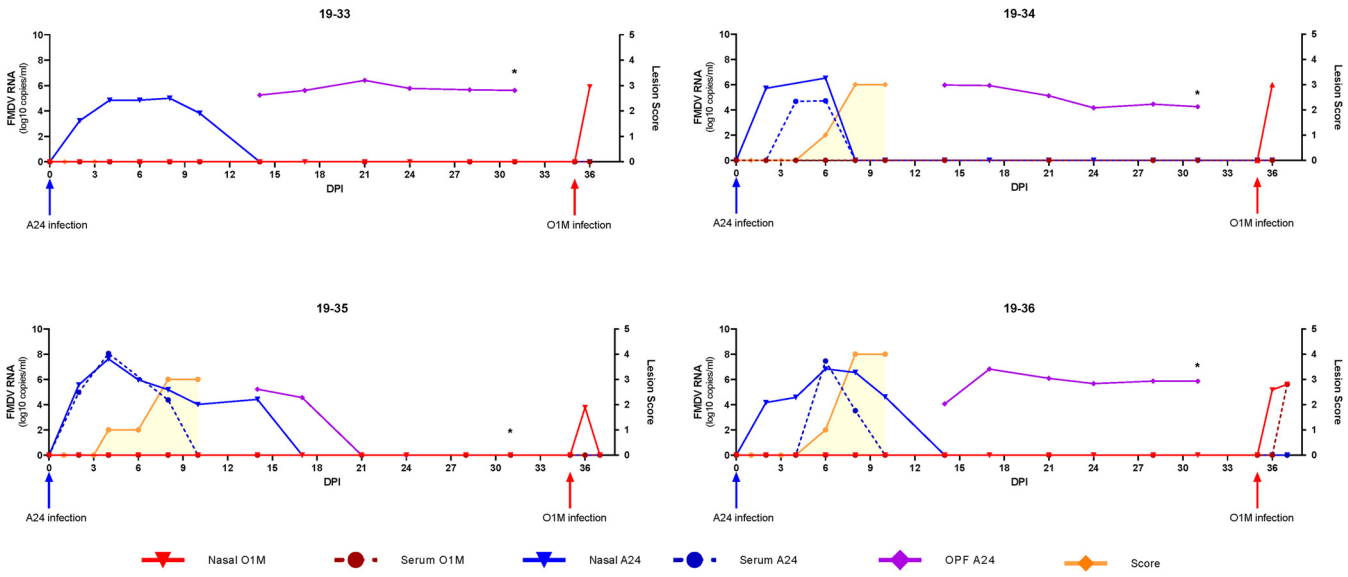

FIG 5 FMDV infection dynamics in cattle that were infected with FMDV A24 Cruzeiro on day 0 and superinfected with FMDV O1 Manisa on day 35. Strain-specific detection of FMDV RNA in nasal swabs (solid lines, triangular markers), sera (hatched lines, circular markers), and OPF (solid purple line, diamond markers) from cattle sequentially infected with FMDV A24 Cruzeiro (blue and purple) and FMDV O1 Manisa (red). Shaded yellow area represents the cumulative lesion score observed through the first 10 days of infection. Animals no. 19-33 and 19-34 (top row) were euthanized for tissue harvest at 1 day post-superinfection, and animals no. 19-35 and 19-36 (bottom row) were euthanized at 2 days post superinfection. Asterisk (*) indicates that OPF samples were collected twice weekly from days 14 to 31.

	24 HPI				48 HPI			
Animal ID	19-09		19-10		19-11		19-12	
Virus strain	A24	O1M	A24	O1M	A24	O1M	A24	O1M
Serum	-	-	-	-	-	5.13	-	-
Tongue						5.91		
Lingual tonsil						4.16		
Palatine tonsil	2.94	+	2.83			+	3.37	+
Ventral soft palate	2.91					+	3.03	3.96
Dorsal soft palate - rostral	2.63	3.96		+	4.85	6	3.31	4.55
Dorsal soft palate - caudal	5.47	6.11		3.53	3.98	5.83	3.59	4.5
Nasopharyngeal tonsil				3.69		+		+
Dorsal nasopharynx - rostral	3.95	4.81	2.59	+	4.59	6.21	5.28	6.15
Dorsal nasopharynx - caudal	3.56	3.92	2.96	+		4.21	4.06	4.95
Lung - distal cranial lobe						4.06		+
Lung - distal middle lobe						4.07		+
Interdigital cleft	3.18		2.93		4.09	5.31		
Coronary band					2.73	3.92	2.56	
Medial retropharyngeal LN	3.98	+	2.63			+		+
Submandibular LN	4.65				2.58	+	3.65	
Popliteal LN	3.46		3.24			+		

FIG 6 FMDV distribution in bovine tissues following FMDV O1 Manisa (red) superinfection, 21 days after initial infection with FMDV A24 Cruzeiro (blue). Strain-specific FMDV detection in tissue samples obtained 24 and 48 h post-FMDV O1 Manisa superinfection. Numbers in table represent $\log_{10}$ GCN/mg of FMDV RNA in tissue or $\log_{10}$ GCN/μL serum for the specific virus. Color gradient indicates increasing FMDV RNA quantities in samples that were positive by both strain-specific qRT-PCR and VI, with virus specificity in VI supernatants determined by strain-specific qRT-PCR. Numbers in uncolored cells indicate quantities of FMDV RNA detected in samples that were negative by virus isolation for that specific virus; plus sign (+) indicates that virus isolation was positive but FMDV RNA content was below the limit of detection.

(ii) Superinfection on 35 dpi. Of the four animals in Group 3, three were determined to have been persistently infected with FMDV A24 based on consistent isolation of infectious virus in OPF samples prior to superinfection. This was consistent with detection of FMDV A24 RNA and infectious FMDV A24 virus in nasopharyngeal tissue samples from these animals collected postmortem. Neither infectious FMDV A24 nor FMDV A24 RNA was found in nasopharyngeal tissue samples from the one animal that had cleared infection (ID no. 19-35; Fig. 7). Consistent with previous findings, low to moderate levels of FMDV A24 RNA were detected, without concurrent detection of infectious FMDV A24, in the lymphoid tissues of these convalescent animals.

FMDV O1M was isolated from nasopharyngeal tissues from all four animals in Group 3, with additional isolation of virus from the lingual tonsil in one individual. There was no isolation of infectious FMDV O1M, nor detection of FMDV O1M RNA, in lungs or lesion predilection sites in any of the animals in this group.

Overall, the distribution of the persistent FMDV A24 virus was more restricted compared to that of the acute/neoteric FMDV O1M virus in all superinfected animals. Interestingly, infectious FMDV O1M was isolated from all tissues in which persistent FMDV A24 virus was detected (Fig. 6 and 7).

Virus localization by immuno-microscopy. The micro-anatomic localization of FMDV in postmortem tissue samples was visualized using multichannel immunofluorescence microscopy and monoclonal antibodies raised against capsid proteins of FMDV serotypes O (27) and A (28), as well as FMDV nonstructural protein 3D (29). As in previous investigations of preclinical and persistent stages of FMDV infection in cattle (8, 9, 16), in all 3 cattle cohorts, FMDV antigen was exclusively detected in the epithelial cells overlaying mucosa-associated lymphoid tissue (follicle-associated epithelium [FAE]) of the nasopharyngeal mucosa. In tissues from simultaneously coinfected animals, approximately equal amounts of FMDV A and FMDV O-positive epithelial cells were found in association with

	24 HPI				48 HPI			
Animal ID	19-33		19-34		19-35		19-36	
Virus strain	A24	O1M	A24	O1M	A24	O1M	A24	O1M
Serum	-	-	-	-	-	-	-	2.16
Tongue								
Lingual tonsil			2.12	3.97				3.7
Palatine tonsil	2.58		2.82		4.22		2.28	+
Ventral soft palate	2.75		2.38					
Dorsal soft palate - rostral	3.87	3.71	3.44	4.18		5.37	2.74	3.73
Dorsal soft palate - caudal	5.95	5.06	5.01	4.42		5.11	3.24	4.57
Nasopharyngeal tonsil		+	2.37	5.62		4.99		+
Dorsal nasopharynx - rostral	4.45	3.8	4.95	5.54		5.95	4.58	6.35
Dorsal nasopharynx - caudal	5.2	5.46	3.16	4.48		4.05	3.03	3.7
Lung - distal cranial lobe								+
Lung - distal middle lobe			2.06					
Interdigital cleft	1.95		2.61					
Coronary band			1.94					
Medial retropharyngeal LN			2.01		3.08	4.14	3.05	3.05
Submandibular LN			4.04		3.39		2.39	2.39
Popliteal LN			4.43		4.59		4.08	4.08

FIG 7 FMDV distribution in bovine tissues following FMDV O1 Manisa (red) superinfection, 35 days after initial infection with FMDV A24 Cruzeiro (blue). Strain-specific FMDV detection in tissue samples obtained 24 and 48 h post-FMDV O1 Manisa superinfection. Numbers in the table represent $\log_{10}$ GCN/mg of FMDV RNA in tissue or $\log_{10}$ GCN/μL serum for the specific virus. Color gradient indicates increasing FMDV RNA quantities in samples that were positive by both strain-specific qRT-PCR and VI, with virus specificity in VI supernatants determined by strain-specific qRT-PCR. Numbers in uncolored cells indicate quantities of FMDV RNA detected in samples that were negative by virus isolation for that specific virus; plus sign (+) indicates that virus isolation was positive but FMDV RNA content was below the limit of detection.

subtle erosions in the surface of the nasopharyngeal mucosa (Fig. 8). In the superinfected cattle that were persistently infected with FMDV A24 and acutely infected with FMDV O1M, there was a disparity in the virus-specific antigen detection, with a markedly greater number of cells being positive for FMDV O antigen compared to those positive for FMDV A antigen. The FMDV O capsid antigen was primarily clustered around epithelial erosions, whereas the FMDV A antigen was localized to clusters of few cells within the surface layer of the FAE (Fig. 9). This discrepancy in the distribution of persistent versus acute infection was further emphasized by a multitude of tissue sections being positive for FMDV O antigen without concurrent detection of FMDV A (Fig. 10). This distribution was similar between the 21-day and 35-day superinfection cohorts. The detection of FMDV 3D protein in the tissue sections is indicative of viral replication. However, because the 3D protein is highly conserved across serotypes, it is not possible to discern from which virus this expression originated.

Virus characterization by deep sequencing. To characterize within-host viral diversity, full-length coding sequences of FMDV were obtained from four anatomically distinct sites of the nasopharyngeal mucosa from all animals. The sample sites analyzed included the rostral and caudal segments of the dorsal surface of the soft palate as well as rostral and caudal segments of the dorsal nasopharynx, which represent consistent sites of both primary and persistent FMDV infection in cattle. One or two biological replicates (corresponding to adjacent pieces of tissue) of each tissue compartment were included in the analyses. Component virus identities were confirmed using Illumina sequencing paired with reference-based read mapping. For most samples, the virus identities obtained through next-generation sequencing (NGS) corresponded to those obtained by qRT-PCR and VI (Fig. 11). While most samples contained the same viruses across biologic replicates and across tissue compartments within each animal, this was not always the case (Fig. 11). Thus, it was found that adjacent tissue segments within the nasopharyngeal mucosa were sometimes infected

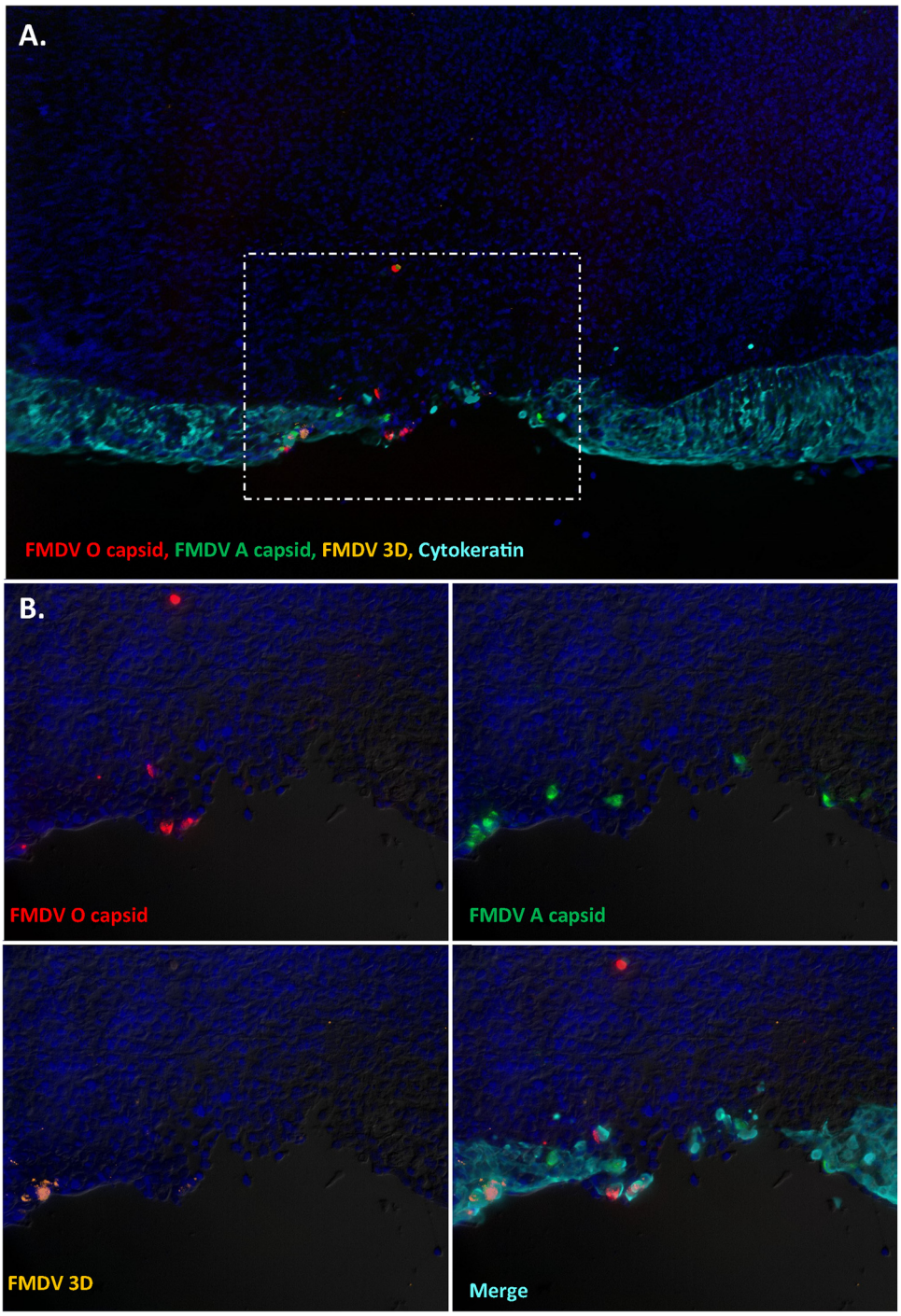

FIG 8 FMDV coinfection in the bovine nasopharyngeal mucosa. (A) FMDV infection in the dorsal nasopharyngeal mucosa at 24 h post-intranasopharyngeal deposition of a mixed inoculum containing equal quantities of FMDV O1 Manisa and FMDV A24 Cruzeiro. (B) FMDV VP1 (O1 Manisa = red, A24 Cruzeiro = green) is localized to cytokeratin+ epithelial cells (teal) within a surface erosion in a segment of follicle-associated epithelium. FMDV 3D protein (orange) was detected in a cluster of a few cells within the same region. There is minimal to no colocalization of FMDV O1M and A24. Panel A = ×10 magnification. Panel B = ×40 magnification with differential interference contrast of region of interest showing separate and merged channels.

with different viruses, corroborating the heterogeneous distribution of infection that was illustrated by immuno-microscopy (Fig. 8 to 10).

Viral sequences were further screened for the existence of interserotypic recombinant FMDVs. This was initially accomplished through the identification of chimeric sequencing

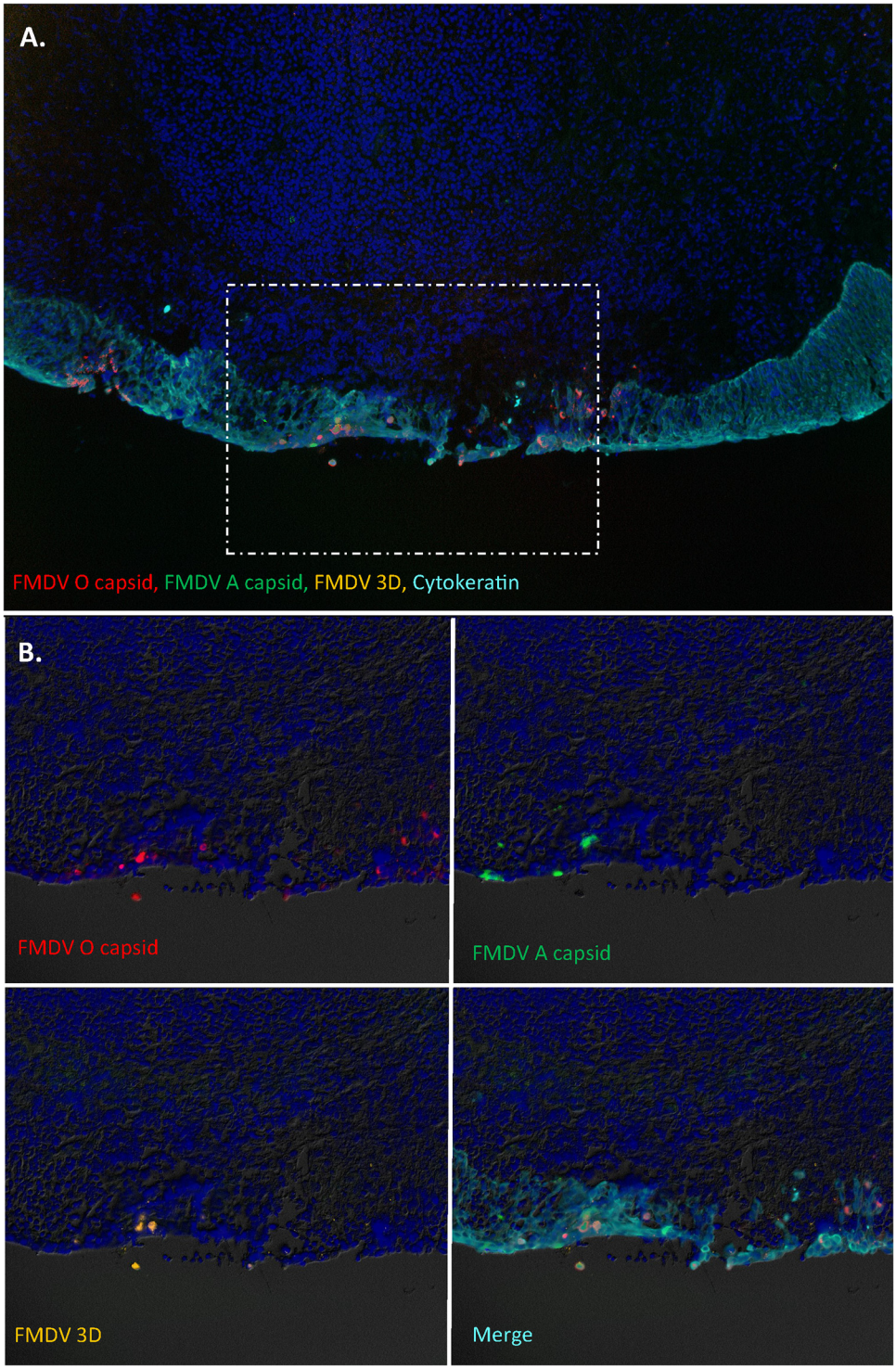

FIG 9 FMDV O1 Manisa superinfection in bovine nasopharynx persistently infected with FMDV A24 Cruzeiro. (A) Early-phase FMDV O1 Manisa infection in the dorsal nasopharyngeal mucosa at 48 h post-FMDV O1 Manisa superinfection of an animal that was persistently infected with FMDV A24 Cruzeiro. (B) FMDV O1 Manisa VP1 (red) is associated with multiple surface erosions within segments of follicle-associated epithelium (cytokeratin = teal). FMDV A24 VP1 (green) is localized to a single cluster of cytokeratin+ epithelial cells directly adjacent to an epithelial erosion. FMDV 3D protein (orange) was detected in a few cells within the same region. Panel A = ×10 magnification. Panel B = ×20 magnification with differential interference contrast of region of interest showing separate and merged channels.

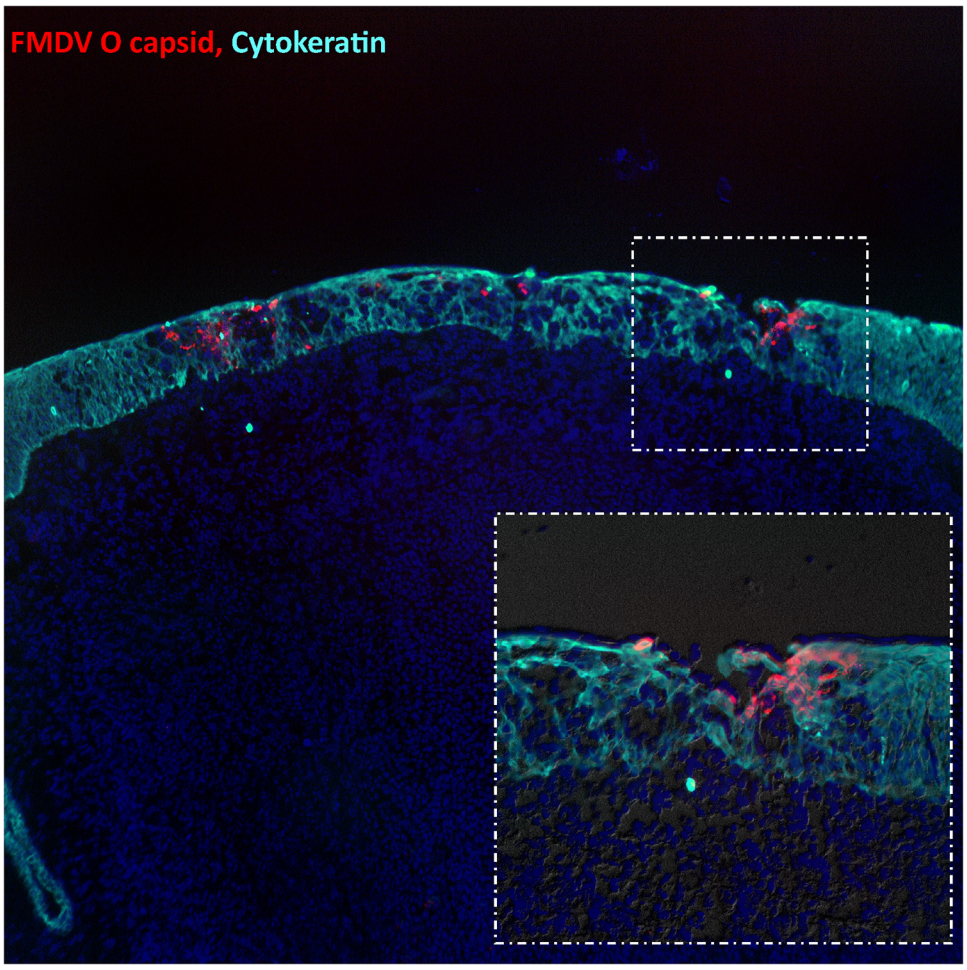

FIG 10 Acute FMDV O1 Manisa infection in the bovine nasopharyngeal mucosa. Multiple foci of FMDV O1 Manisa (red) infection associated with erosions within the mucosal surface of the dorsal soft palate at 48 h postinfection. The VP1 antigen is exclusively detected within cytokeratin+ (teal) cells within segments of follicle-associated epithelium. Image = ×10 magnification. Inset: ×40 magnification with differential interference contrast of region of interest.

reads. In brief, reads which mapped similarly to both the FMDV A24 and FMDV O1M reference genomes (i.e., chimeric reads) were extracted and then re-mapped to each reference genome. Chimeric reads indicating shared breakpoints were identified across different nasopharyngeal tissue samples and replicates from animals no. 19-34 (breakpoint in 2B coding region) and 19-36 (breakpoint in 3D coding region) (Fig. 12). Suspect recombinants were detected at very low levels (<1%) in the dorsal nasopharynx and rostral and caudal segments of the dorsal soft palate of animal no. 19-34 (24 hpi), as well as in the dorsal nasopharynx of animal no. 19-36 (48 hpi). In contrast, a recombinant virus estimated to comprise approximately 21% of sequenced genomes was detected in a dorsal soft palate sample of animal no. 19-36 (48 hpi). Specifically, this sample included full-length FMDV O1M, but also a segment from the center of the 3D coding region through the 3′ UTR (untranslated region) derived from the FMDV A24 genome (breakpoint 7,441 to 7,460 on the FMDV O1M reference genome) (Fig. 12). To confirm the presence of the recombinant in this sample, plaque purification was performed and a total of 15 resultant plaque isolates were successfully Illumina sequenced. Of the 15 sequenced plaque isolates, 4 included pure interserotypic FMDV O1M-A24 recombinants with breakpoints precisely matching the predicted recombinant.

DISCUSSION

We have previously shown that persistently infected FMDV carrier cattle became clinically or subclinically superinfected when exposed to a heterologous FMDV strain

Group	Time point	Animal ID	Tissue compartment: Dorsal soft palate (rostral)	Dorsal soft palate (caudal)	Dorsal Nasopharyx (rostral)	Dorsal Nasopharyx (caudal)
Group 1: Simultaneous co-infection	24 HPI	19-01	O/A	O/A	O/A	O/A
		19-02	O/A	O/A	O/A	O/A
	48 HPI	19-03	O/A	O/A	O/A	O/A
		19-04	O/A	O/A	O/A	O/A
Group 2: A24= 0 dpi, O1M= 21dpi	24 HPI	19-09	O	O/A | O	O	O
		19-10	O	O	O/A | O	O
	48 HPI	19-11	O	O/A	O/A | O	O
		19-12	O	O	O	O
Group 3: A24= 0 dpi, O1M= 35dpi	24 HPI	19-33	O/A	O/A | O	O/A | A	O/A
		19-34	O/A	O/A	O/A	O/A
	48 HPI	19-35	O	O	O	O
		19-36	O	O/Recomb** | O	O/Recomb*	O/A | O

* Recombinant <1% of virus population
**Recombinant ca 20% of virus population

FIG 11 Characterization of FMDV infection by next-generation sequencing (NGS) in distinct compartments of the bovine nasopharynx. Viruses isolated from four distinct compartments of the nasopharynx: rostral and caudal segments of the dorsal surface of the soft palate as well as rostral and caudal segments of the dorsal nasopharynx were analyzed by NGS. All samples obtained from simultaneously infected animals (Group 1) contained both viruses (purple cells). In animals which had been superinfected with FMDV O1 Manisa 21 or 35 days post-infection with FMDV A24 (Groups 2 and 3), FMDV O1 Manisa (red cells) had a wider distribution compared to FMDV A24. Only one tissue replicate contained FMDV A24 without concurrent detection of FMDV O1M (blue cell). Split cells of different color designations indicate that different viruses, or combinations of viruses, were detected in replicate samples within the same anatomic compartment. Asterisk(*) indicates that samples from animal no. 19-36 contained an interserotypic recombinant virus which was confirmed through plaque purification and analysis of plaques by NGS.

and that interserotypic recombinants could be detected in oropharyngeal fluid samples as early as 10 days after superinfection (26, 30). Our current investigation describes the detailed infection dynamics and tissue distribution of viruses in cattle that were euthanized for postmortem tissue harvest during the early stages of simultaneous coinfection or staggered superinfection.

The earliest isolation of interserotypic recombinants was at 48 h after superinfection, with additional suspected low-level recombinants detected in a different animal as early as 24 h. Recombination among FMDV strains has been described under natural and experimental conditions (12–14, 26); however, the specific mechanisms of occurrence and emergence (e.g., timing and anatomic site) have not been described. The current findings further emphasize the frequency at which FMDV recombination occurs in superinfected carrier animals, which may have important implications for FMDV molecular epidemiology. The lack of detection of recombinant genomes in samples from the simultaneously coinfected cohort is similar to our previous findings (26) and suggests that this form of coinfection may not be a relevant condition for FMDV recombination. This distinction is specifically noteworthy in this study because the micro-anatomic distributions of the two viruses were essentially identical across cohorts, with distinct viruses detected in adjacent epithelial cells within the nasopharyngeal mucosa.

It has been shown *in vitro* that FMDV recombination will occur in any cell that is simultaneously infected with different virus variants (31–33). However, the mechanisms and frequencies of the generation of detectable levels of recombinant viruses in infected animals are not known. Acute FMDV infection induces an immediate cellular antiviral response (34, 35). It can thus be speculated that a cell which has recently been infected by one FMDV may be resistant to infection by a similar or different virus for

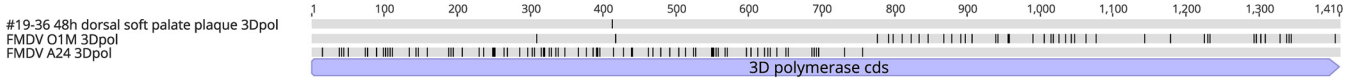

FIG 12 Schematic of the interserotypic recombinant FMDV genome isolated from the dorsal soft palate of animal no. 19-36, obtained 48 h post-FMDV O1M superinfection. The virus identified in four sequenced plaques was comprised of an FMDV O1M-derived genome from the 5′ UTR through the center of the 3D coding region and an FMDV A24-derived coding region from the mid-3D through the 3′ UTR. In each alignment, horizontal rows colored light grey indicate identity with the reference sequence while black banding indicates dissimilarity.

some time thereafter. Persistent FMDV infection, in contrast, is not associated with an induced antiviral state, but with potential downregulation of antiviral pathways (36, 37). However, high levels of systemic and secreted anti-FMDV antibodies are present in carriers as well as in convalescent animals that have successfully cleared infection (21, 38, 39). Even though the distribution of persistent FMDV infection is limited to a distinct population of cells within the nasopharyngeal mucosa, it is possible that these cells are highly susceptible to FMDV superinfection based both on their distinctly permissive phenotype and the downregulation of antiviral pathways. Although visualization of the two distinct viruses within the same cell by immunofluorescence was not accomplished, the molecular detection of recombinant viruses demonstrates that cellular-level coinfection must have occurred. As in our previous findings (26, 30), the recombinants found in the current study had capsid-coding regions derived from the superinfecting FMDV O1M virus. Such recombinants may have an immunological advantage over the persistently infecting FMDV A24 virus because the superinfected animals will initially not have antibodies against FMDV O1M capsid. Our previous work demonstrated that there was no cross-neutralization of the FMDV O1M virus by sera obtained from the FMDV A24-infected animals prior to the superinfection (26). However, lack of serum neutralizing capacity does not explain any advantage the recombinant viruses, with FMDV O-derived capsids and FMDV A-derived nonstructural coding regions, would have in relation to the parental FMDV O1M viruses. Thus, the relative success of these recombinants is likely associated with other aspects of viral fitness that are still unknown.

The interserotypic recombinant isolated in this investigation was obtained from an animal that was superinfected with FMDV O1M at 35 days postinfection with FMDV A24. Although there was no isolation of recombinant viruses from the 21-day superinfection cohort in the current investigation, our previous work demonstrated frequent isolation of recombinant viruses in OPF samples obtained from carriers superinfected at 21 dpi (26). Whereas the recombinant virus isolated in the current investigation had a breakpoint within the 3D coding region, our previously published study demonstrated breakpoints within other nonstructural coding regions (26, 30). Similar for both investigations was the complete lack of detection of any recombinant viruses in any samples from simultaneously coinfected cohorts.

In the superinfected cattle, there was a heterogeneous distribution of viruses across the distinct regions of the nasopharyngeal mucosa. Specifically, samples from adjacent regions, and even biological replicates from within the same region, occasionally contained viruses of distinct serotypes or combinations of serotypes. Our previous studies have shown that FMDV selectively infects specific segments of epithelium within the bovine nasopharynx during both primary and persistent stages of infection (8, 9, 16, 17, 40). The same studies also indicated that microscopic identification of foci of FMDV infection in the nasopharynx is exceedingly rare and minute, further suggesting an uneven distribution of infection within the specific anatomic region. Combined, these findings suggest that FMDV infection of the bovine upper respiratory tract is multifocal, and that distinct foci of infection may contain viruses that could potentially evolve independently over time. OPF samples obtained through scraping of the mucosal surface using a probang cup (11, 15) are likely representative of a larger mucosal surface area, which is supported by frequent detection of mixed virus populations in such samples (41).

The epidemiological relevance of FMDV carrier cattle is still controversial, yet generally assumed to be negligible due to the seemingly low level of contagion associated with these animals (23, 42). Conflicting evidence includes the known presence of infectious virus within the pharynx of carriers (10, 11) and the demonstrated transmissibility of FMDV via OPF harvested from carriers (10, 20). However, superinfected carriers comprise a distinct category of animals because these individuals are concurrently persistently and acutely infected. Despite the possible absence of clinical FMD signs, the neoteric (early) phase of subclinical FMDV infection differs from the persistent phase of

infection because viral shedding can often be detected in nasal swab samples (16). Although it was not possible to assess the clinical outcomes of superinfection in the animals included in the current investigation, the detection of recombinant viruses as early as 24 to 48 hpi confirms that such recombinants were present during the early phase of infection when virus shedding is most substantial.

The extensive diversity of FMDV is well-known, yet the sources and mechanisms of the continuance of that diversity are incompletely understood across scales ranging from the individual animal to the population. The similar micro-anatomic localization of primary and persistent FMDV infection in cattle creates an environment which may facilitate both the generation and propagation of novel recombinant virus strains, as demonstrated in the current work. Under standard surveillance methods, superinfected FMDV carriers remain largely undetected because field sampling is typically based on the presence of suspect FMD lesions. Similarly, recombinant FMDV strains will not be detected when genomic surveillance is based on VP1 sequencing alone. Thus, further research is required to assess the prevalence and potential transmission risk associated with superinfected FMDV carrier cattle and other ruminant species. Improved understanding of the mechanisms and relevance of the distinct forms of subclinical FMDV infection will ultimately contribute to rational methods of FMDV control and elimination in regions of endemicity and following outbreaks in FMD-free regions.

MATERIALS AND METHODS

Viruses. The two viruses used in this study were bovine-derived strains of FMDV A24 Cruzeiro and FMDV O1 Manisa. The pathogenesis of both viruses has been previously characterized in cattle using the same inoculation system and dosage used in the current study (8, 16, 43). FMDV is considered a Tier 1 select agent in the United States. All work described here was performed within biosafety level 3 (BSL3) or BSL3Ag laboratory facilities at the Plum Island Animal Disease Center (PIADC), New York, in accordance with national and institutional policies overseen by the PIADC Biosafety and Select Agent Program Office.

Animals and animal experiments. The current investigation was based on two separate experimental studies. All experimental procedures were approved by the PIADC institutional animal care and usage committee (protocol no. 209-17-R) which ensures humane and ethical treatment of animals. The cattle were approximately 10-month-old Holstein heifers procured from a USDA-certified vendor.

Study design. The 12 animals used for this investigation were part of a large-scale study of heterologous FMDV coinfection and recombination. The overarching study design, as well as clinical outcomes and viral dynamics in animals observed through 28 to 70 days, have been previously reported (26). In brief, three groups of four cattle each were exposed to 10^6 $TCID_{50}$ each of FMDV A24 and FMDV O1M through intranasopharyngeal deposition (43). Group 1 was simultaneously infected with both virus strains in a mixed inoculum, Group 2 was initially infected with FMDV A24 on day 0 and superinfected with FMDV O1M on study day 21, and Group 3 was initially infected with FMDV A24 on day 0 and superinfected with FMDV O1M on day 35 (Fig. 1). Two animals from each study group were euthanized for tissue harvest at 24 and 48 h after the final (or combined) virus exposure.

Clinical evaluation and antemortem sample collection. Jugular vein blood samples and nasal swabs were collected at 0, 24, and 48 hpi from the simultaneously infected study group. From Groups 2 and 3, nasal swabs and blood samples were collected every other day from days 0 through 10. Sample collection from 14 days after the first virus inoculation until the superinfection consisted of weekly blood sampling and twice-weekly collection of nasal swabs and OPF by probang sampling (11, 15). After the superinfection, nasal swabs and blood were collected at 24-h intervals until euthanasia. Nasal swabs and whole blood samples were centrifuged to extract nasal fluid and sera. OPF samples were homogenized using 6′′/16G steel cannulas attached to 20-mL syringes as previously described (16). One aliquot of OPF designated for virus isolation was treated with 1,1,2-trichlorotrifluoroethane (TTE) to dissociate virus-antibody complexes prior to freezing (16, 44). All samples were stored at −70°C until further processing.

Clinical examinations were performed approximately every other day from 0 to 10 days after the initial virus inoculation and at the time of euthanasia. Cattle were sedated by intramuscular injection of xylazine hydrochloride (0.66 mg/kg) to enable thorough examination of the feet and oral cavities. Sedation was reversed by intravenous injection of tolazoline (2.0 mg/kg). The progression of clinical infection (lesion distribution) was measured by a quantitative cumulative scoring system. In brief, any vesicular lesions observed within the oral cavity (dental pad, tongue, gingiva), lips, or nostrils counted for 1 point, with additional points added for vesicles on any of the four feet (1 point per foot), resulting in a maximum possible score of 5.

Postmortem sample collection. Study animals were sedated by intramuscular injection of xylazine hydrochloride and euthanized by intravenous injection of an overdose of pentobarbital. Necropsies with tissue sample harvest were performed immediately following euthanasia. A predetermined list of 16 distinct anatomic sites were sampled (Fig. 2 to 4). Sampled tissues were selected based on accumulated knowledge of FMDV tissue distribution from previous studies (8, 9, 16, 17) and represented the upper and lower respiratory tracts (nasopharynx and lungs), oral- and oropharyngeal cavities, lymph nodes

associated with FMDV lesion predilection sites, and skin from the coronary bands and interdigital clefts (Fig. 2 to 4). Each sampled tissue was divided into multiple ca. 30-mg aliquots that were placed in individual tubes before being frozen over liquid nitrogen. An adjacent specimen from each tissue was divided into replicates, embedded in optimal cutting temperature medium (Sakura Finetek, Torrance, CA), placed in cryomolds, and frozen over liquid nitrogen. Tissue samples were kept frozen in the vapor phase over liquid nitrogen and transferred to the lab within 2 h after collection for storage at −70°C until further processing.

FMDV RNA detection. Two aliquots of each tissue sample collected at necropsy were thawed and individually macerated in tissue culture medium using a TissueLyser bead beater (Qiagen, Valencia, CA) and stainless steel beads (Qiagen cat. no. 69989). Total RNA was extracted from tissue macerates, serum, nasal swabs, and OPF samples using Ambion's MagMax-96 Viral RNA isolation kit (Ambion, Austin, TX) on a King Fisher-96 Magnetic Particle Processor (Thermo Fisher Scientific, Waltham, MA). All tissue macerates, sera, nasal fluid, and OPF samples were analyzed using qRT-PCR targeting the 3D region of the FMDV genome (45), with forward and reverse primers adapted from Rasmussen et al. (46) and chemistry and cycling conditions as previously described (47). Additionally, two strain-specific qRT-PCR systems with primers and probes targeting the capsid coding regions were used to differentiate between the two viruses in this study (26). All assays were run in parallel, with the extracted RNA analyzed simultaneously using the three detection systems. Cycle threshold (C_T) values of <38 were considered positive. Cycle threshold values were converted to RNA copies per mL or mg using an equation derived from analysis of serial 10-fold dilutions of *in vitro*-synthesized, strain-specific FMDV RNA of known concentration. The equations of the curve of RNA copy numbers versus C_T values were further adjusted for the average mass of tissue samples and the specific dilutions used during sample processing.

Virus isolation. Aliquots of all macerated tissue samples and TTE-treated probang samples were cleared of debris and potential bacterial contamination by centrifugation through Spin-X filter columns (pore size 0.45 μm, Sigma-Aldrich). Virus isolation was performed using LFBK-αvβ6 cells (48, 49) following a previously described protocol (50). The presence of amplified FMDV in VI supernatants was confirmed by qRT-PCR (universal and strain-specific systems).

FMDV sequence acquisition. FMDV sequence data were obtained from all OPF and nasopharyngeal tissue samples from which FMDV could be isolated on LFBK-αVβ6 cells using previously described methodology (26). In brief, RNA was extracted from VI supernatants as described above. Samples were reverse-transcribed using the Superscript II First-Strand Synthesis System (Invitrogen) with random hexameric primers. Each sample was run in duplicate, with one reverse-transcription reaction of each sample also including two 5′-oriented FMDV-specific primers targeting the 3′ UTR (5′-ACGCTCGACA TTTTTTTTTTTTTTT) and the 2A coding region (5′-GCCCRGGGTTGGACTC). Double-stranded (ds)-cDNA was generated using the NEBNext Ultra II Nondirectional RNA Second-Strand Synthesis module (New England BioLabs, Ipswich, MA) and purified with SPRIselect beads (Beckman Coulter, Brea, CA). The sequencing library was prepared using the Nextera XT DNA Library Preparation kit (Illumina, San Diego, CA) and sequenced on the NextSeq 550 platform with the 300-cycle kit (2 × 150-bp, paired-end). Reads were trimmed and filtered for quality (settings: quality limit = 0.03, maximum ambiguous nucleotides = 2), including removal of the FMDV-specific primers, and competitively assembled to references A24 Cruzeiro (GenBank accession no. AY593768) and O1 Manisa (GenBank no. AY593823) in CLC Genomics Workbench 12.X and 20.X (Qiagen). A minimum coverage of 10 reads was required for base calls; however, for the vast majority of sites, coverage far exceeded 1,000× reads per site.

Chimeric read analysis was performed as detailed by Arzt et al. (26). In brief, trimmed reads which aligned equally well to both the FMDV A24 and FMDV O1M reference genomes were collected and separately re-mapped to each reference. Re-mapped reads encoding chimeric nucleotide identity (~1:1 ratio of FMDV A24:FMDV O1M or FMDV O1M:FMDV A24) were corroborated across technical replicates and neighboring tissue isolates. Separately passaged nasopharyngeal tissues from animal no. 19-36 (48 hpi) included evidence of interserotypic recombinant viruses alongside the majority of FMDV O1M non-recombinant virus (Fig. 11). Specifically, for each of these samples, reads belonging to the full FMDV O1M genome were present with very high coverage (>1,000 reads per site), while reads belonging to the FMDV-A genome covered approximately half of the 3D coding region and the 3′ UTR. The concordance across these three samples strongly suggested the existence of an interserotypic recombinant comprised of an FMDV O1M-derived genome from the 5′ UTR through approximately half of the 3D coding region and an FMDV A24-derived genome from that putative breakpoint in 3D through the 3′ UTR. The relative abundance of this interserotypic recombinant in the caudal segment of the dorsal soft palate sample from animal no. 19-36 was estimated to be ~21%. Plaque isolation was performed to purify the recombinant identified in the dorsal soft palate sample from animal 19-36, as detailed previously (30). In brief, serial dilutions of the macerated sample were inoculated on LFBK-αvβ6 cells (48, 51) and incubated for 48 h. Discrete plaques were picked and directly fed into the Illumina-sequencing pipeline described above. Similarly, the sequencing of separately passaged pharyngeal tissue from animal 19-34 included low-level evidence of recombinants with breakpoints within coding region 2B. However, the proportion of recombinant viruses compared to non-recombinant parental strains in each sample was estimated to be too low to confirm through plaque isolation.

Immuno-microscopy. After screening of tissue samples for FMDV RNA and infectious virus by qRT-PCR and VI, respectively, detection of antigen in cryosections by immunohistochemistry (IHC) and multichannel immunofluorescence (MIF) was performed as previously described (9, 52). Slides were examined with a wide-field epifluorescence microscope, and images were captured with a cooled, monochromatic digital camera. Images of individual detection channels were adjusted for contrast and brightness and merged in commercially available software (Adobe Photoshop CC; Adobe Inc., San Jose, CA). Alternate

sections of analyzed tissues were included as isotype controls, and additional negative-control tissue sections were prepared from corresponding tissues derived from non-infected cattle. FMDV structural protein VP1 was detected using mouse monoclonal antibody 6HC4 for FMDV A24, and 10GA4 for FMDV O1M (27, 28). Nonstructural FMDV 3D protein was detected using the mouse monoclonal antibody F19-6 (29). MIF experiments also included labeling of epithelial cytokeratin using rabbit anti-cytokeratin (Life Technologies cat no. 180059), as well as isotype control antibodies for the anti-FMDV antibodies corresponding to mouse IgG1, IgG2b, and IgG3 (Invitrogen cat no. MG100, MG2B00, and MG300).

Data availability. Data have been deposited in the National Center for Biotechnology Information's Sequence Read Archive (SRA) under BioProject ID no. PRJNA662932.

ACKNOWLEDGMENTS

We thank Drs. Rachel M. Palinski and Miranda R. Bertram for help with animal experiments and Dr. Juergen Richt for scientific input. Ethan J. Hartwig and George R. Smoliga are thanked for ecellent technical support and sample processing.

This work was funded through U.S. Department of Agriculture, Agricultural Research Service Current Research Information System Project no. 1940-32000-061-00D. Haillie Meek was supported through a Plum Island Animal Disease Center Research Participation Program fellowship administered by the Oak Ridge Institute for Science and Education (ORISE) through an inter-agency agreement with the U.S. Department of Energy.

REFERENCES

1. Grubman MJ, Baxt B. 2004. Foot-and-mouth disease. Clin Microbiol Rev 17:465–493. https://doi.org/10.1128/CMR.17.2.465-493.2004.
2. Office International des Epizooties (OIE). 2022. Application for official recognition by the OI of free status for foot-and-mouth disease virus. *In* Terrestrial Animal Health Code. Available from https://www.woah.org/fileadmin/Home/eng/Health_standards/tahc/current/chapitre_selfdeclaration_FMD.pdf. WOAH, Paris, France.
3. Shanafelt DW, Perrings CA. 2017. Foot and mouth disease: the risks of the international trade in live animals. Rev Sci Tech 36:839–865. https://doi.org/10.20506/rst.36.3.2719.
4. Knight-Jones TJ, Rushton J. 2013. The economic impacts of foot and mouth disease: what are they, how big are they and where do they occur? Prev Vet Med 112:161–173. https://doi.org/10.1016/j.prevetmed.2013.07.013.
5. Knight-Jones TJ, McLaws M, Rushton J. 2017. Foot-and-mouth disease impact on smallholders: what do we know, what don't we know and how can we find out more? Transbound Emerg Dis 64:1079–1094. https://doi.org/10.1111/tbed.12507.
6. Knowles NJ, Samuel AR. 2003. Molecular epidemiology of foot-and-mouth disease virus. Virus Res 91:65–80. https://doi.org/10.1016/s0168-1702(02)00260-5.
7. Doel TR. 1996. Natural and vaccine-induced immunity to foot and mouth disease: the prospects for improved vaccines. Rev Sci Tech 15:883–911. https://doi.org/10.20506/rst.15.3.955.
8. Stenfeldt C, Eschbaumer M, Pacheco JM, Rekant SI, Rodriguez LL, Arzt J. 2015. Pathogenesis of primary foot-and-mouth disease virus infection in the nasopharynx of vaccinated and non-vaccinated cattle. PLoS One 10:e0143666. https://doi.org/10.1371/journal.pone.0143666.
9. Stenfeldt C, Hartwig EJ, Smoliga GR, Palinski R, Silva EB, Bertram MR, Fish IH, Pauszek SJ, Arzt J. 2018. Contact challenge of cattle with foot-and-mouth disease virus validates the role of the nasopharyngeal epithelium as the site of primary and persistent infection. mSphere 3:e00493-18. https://doi.org/10.1128/mSphere.00493-18.
10. Sutmoller P, McVicar JW, Cottral GE. 1968. The epizootiological importance of foot-and-mouth disease carriers. I. Experimentally produced foot-and-mouth disease carriers in susceptible and immune cattle. Arch Gesamte Virusforsch 23:227–235. https://doi.org/10.1007/BF01241895.
11. Sutmoller P, Gaggero A. 1965. Foot-and mouth diseases carriers. Vet Rec 77:968–969.
12. Brito B, Pauszek SJ, Hartwig EJ, Smoliga GR, Vu LT, Dong PV, Stenfeldt C, Rodriguez LL, King DP, Knowles NJ, Bachanek-Bankowska K, Long NT, Dung DH, Arzt J. 2018. A traditional evolutionary history of foot-and-mouth disease viruses in Southeast Asia challenged by analyses of non-structural protein coding sequences. Sci Rep 8:6472. https://doi.org/10.1038/s41598-018-24870-6.
13. Bachanek-Bankowska K, Di Nardo A, Wadsworth J, Mioulet V, Pezzoni G, Grazioli S, Brocchi E, Kafle SC, Hettiarachchi R, Kumarawadu PL, Eldaghayes IM, Dayhum AS, Meenowa D, Sghaier S, Madani H, Abouchoaib N, Hoang BH, Vu PP, Dukpa K, Gurung RB, Tenzin S, Wernery U, Panthumart A, Seeyo KB, Linchongsubongkoch W, Relmy A, Bakkali-Kassimi L, Scherbakov A, King DP, Knowles NJ. 2018. Reconstructing the evolutionary history of pandemic foot-and-mouth disease viruses: the impact of recombination within the emerging O/ME-SA/Ind-2001 lineage. Sci Rep 8:14693. https://doi.org/10.1038/s41598-018-32693-8.
14. Jamal SM, Nazem Shirazi MH, Ozyoruk F, Parlak U, Normann P, Belsham GJ. 2020. Evidence for multiple recombination events within foot-and-mouth disease viruses circulating in West Eurasia. Transbound Emerg Dis 67:979–993. https://doi.org/10.1111/tbed.13433.
15. Stenfeldt C, Arzt J. 2020. The carrier conundrum; a review of recent advances and persistent gaps regarding the carrier state of foot-and-mouth disease virus. Pathogens 9:167. https://doi.org/10.3390/pathogens9030167.
16. Stenfeldt C, Eschbaumer M, Rekant SI, Pacheco JM, Smoliga GR, Hartwig EJ, Rodriguez LL, Arzt J. 2016. The foot-and-mouth disease carrier state divergence in cattle. J Virol 90:6344–6364. https://doi.org/10.1128/JVI.00388-16.
17. Arzt J, Pacheco JM, Rodriguez LL. 2010. The early pathogenesis of foot-and-mouth disease in cattle after aerosol inoculation: identification of the nasopharynx as the primary site of infection. Vet Pathol 47:1048–1063. https://doi.org/10.1177/0300985810372509.
18. Cortey M, Ferretti L, Perez-Martin E, Zhang F, de Klerk-Lorist LM, Scott K, Freimanis G, Seago J, Ribeca P, van Schalkwyk L, Juleff ND, Maree FF, Charleston B. 2019. Persistent infection of African buffalo (*Syncerus caffer*) with foot-and-mouth disease virus: limited viral evolution and no evidence of antibody neutralization escape. J Virol 93:e00563-19. https://doi.org/10.1128/JVI.00563-19.
19. Maree F, de Klerk-Lorist LM, Gubbins S, Zhang F, Seago J, Perez-Martin E, Reid L, Scott K, van Schalkwyk L, Bengis R, Charleston B, Juleff N. 2016. Differential persistence of foot-and-mouth disease virus in African buffalo is related to virus virulence. J Virol 90:5132–5140. https://doi.org/10.1128/JVI.00166-16.
20. Arzt J, Belsham GJ, Lohse L, Botner A, Stenfeldt C. 2018. Transmission of foot-and-mouth disease from persistently infected carrier cattle to naive cattle via transfer of oropharyngeal fluid. mSphere 3:e00365-18. https://doi.org/10.1128/mSphere.00365-18.
21. Parthiban AB, Mahapatra M, Gubbins S, Parida S. 2015. Virus excretion from foot-and-mouth disease virus carrier cattle and their potential role in causing new outbreaks. PLoS One 10:e0128815. https://doi.org/10.1371/journal.pone.0128815.
22. Ilott MC, Salt JS, Gaskell RM, Kitching RP. 1997. Dexamethasone inhibits virus production and the secretory IgA response in oesophageal-pharyngeal fluid in cattle persistently infected with foot-and-mouth disease virus. Epidemiol Infect 118:181–187. https://doi.org/10.1017/s0950268896007376.
23. Bertram M, Vu LT, Pauszek JR, Brito B, Hartwig E, Smoliga G, Hoang BH, Phuong NT, Stenfeldt C, Fish IH, Hung VV, Delgado A, VanderWaal K, Rodriguez LL, Long NT, Dung DH, Arzt J. 2018. Lack of transmission of foot-and-mouth disease virus from persistently infected cattle to naïve

cattle under field conditions in Vietnam. Front Vet Sci 5:174. https://doi.org/10.3389/fvets.2018.00174.
24. WOAH. 2022. Infection with foot and mouth disease virus. *In* Terrestrial animal health code. Available from https://www.woah.org/fileadmin/Home/eng/Health_standards/tahc/current/chapitre_fmd.pdf. Accessed July 14, 2016. WOAH, Paris, France.
25. Barnett PV, Geale DW, Clarke G, Davis J, Kasari TR. 2015. A review of OIE country status recovery using vaccinate-to-live versus vaccinate-to-die foot-and-mouth disease response policies I: benefits of higher potency vaccines and associated NSP DIVA test systems in post-outbreak surveillance. Transbound Emerg Dis 62:367–387. https://doi.org/10.1111/tbed.12166.
26. Arzt J, Fish IH, Bertram MR, Smoliga GR, Hartwig EJ, Pauszek SJ, Holinka-Patterson L, Diaz-San Segundo FC, Sitt T, Rieder E, Stenfeldt C. 2021. Simultaneous and staggered foot-and-mouth disease virus coinfection of cattle. J Virol 95:e0165021. https://doi.org/10.1128/JVI.01650-21.
27. Stave JW, Card JL, Morgan DO. 1986. Analysis of foot-and-mouth disease virus type O1 Brugge neutralization epitopes using monoclonal antibodies. J Gen Virol 67:2083–2092. https://doi.org/10.1099/0022-1317-67-10-2083.
28. Baxt B, Vakharia V, Moore DM, Franke AJ, Morgan DO. 1989. Analysis of neutralizing antigenic sites on the surface of type A12 foot-and-mouth disease virus. J Virol 63:2143–2151. https://doi.org/10.1128/JVI.63.5.2143-2151.1989.
29. Yang M, Clavijo A, Li M, Hole K, Holland H, Wang H, Deng MY. 2007. Identification of a major antibody binding epitope in the non-structural protein 3D of foot-and-mouth disease virus in cattle and the development of a monoclonal antibody with diagnostic applications. J Immunol Methods 321:174–181. https://doi.org/10.1016/j.jim.2007.01.016.
30. Fish I, Stenfeldt C, Spinard E, Medina GN, Azzinaro PA, Bertram MR, Holinka L, Smoliga GR, Hartwig EJ, de Los Santos T, Arzt J. 2022. Foot-and-mouth disease virus interserotypic recombination in superinfected carrier cattle. Pathogens 11:644. https://doi.org/10.3390/pathogens11060644.
31. King AM, McCahon D, Slade WR, Newman JW. 1982. Recombination in RNA. Cell 29:921–928. https://doi.org/10.1016/0092-8674(82)90454-8.
32. King AM, McCahon D, Slade WR, Newman JW. 1982. Biochemical evidence of recombination within the unsegmented RNA genome of aphthovirus. J Virol 41:66–77. https://doi.org/10.1128/JVI.41.1.66-77.1982.
33. Kirkegaard K, Baltimore D. 1986. The mechanism of RNA recombination in poliovirus. Cell 47:433–443. https://doi.org/10.1016/0092-8674(86)90600-8.
34. Li K, Wang C, Yang F, Cao W, Zhu Z, Zheng H. 2021. Virus-host interactions in foot-and-mouth disease virus infection. Front Immunol 12:571509. https://doi.org/10.3389/fimmu.2021.571509.
35. Medina GN, Segundo FD, Stenfeldt C, Arzt J, de Los Santos T. 2018. The different tactics of foot-and-mouth disease virus to evade innate immunity. Front Microbiol 9:2644. https://doi.org/10.3389/fmicb.2018.02644.
36. Eschbaumer M, Stenfeldt C, Smoliga GR, Pacheco JM, Rodriguez LL, Li RW, Zhu J, Arzt J. 2016. Transcriptomic analysis of persistent infection with foot-and-mouth disease virus in cattle suggests impairment of apoptosis and cell-mediated immunity in the nasopharynx. PLoS One 11:e0162750. https://doi.org/10.1371/journal.pone.0162750.
37. Stenfeldt C, Eschbaumer M, Smoliga GR, Rodriguez LL, Zhu J, Arzt J. 2017. Clearance of a persistent picornavirus infection is associated with enhanced pro-apoptotic and cellular immune responses. Sci Rep 7:17800. https://doi.org/10.1038/s41598-017-18112-4.
38. Stenfeldt C, Heegaard PM, Stockmarr A, Tjornehoj K, Belsham GJ. 2011. Analysis of the acute phase responses of serum amyloid A, haptoglobin and type 1 interferon in cattle experimentally infected with foot-and-mouth disease virus serotype O. Vet Res 42:66. https://doi.org/10.1186/1297-9716-42-66.
39. Eschbaumer M, Stenfeldt C, Rekant SI, Pacheco JM, Hartwig EJ, Smoliga GR, Kenney MA, Golde WT, Rodriguez LL, Arzt J. 2016. Systemic immune response and virus persistence after foot-and-mouth disease virus infection of naive cattle and cattle vaccinated with a homologous adenovirus-vectored vaccine. BMC Vet Res 12:205. https://doi.org/10.1186/s12917-016-0838-x.
40. Stenfeldt C, Arzt J, Pacheco JM, Gladue DP, Smoliga GR, Silva EB, Rodriguez LL, Borca MV. 2018. A partial deletion within foot-and-mouth disease virus non-structural protein 3A causes clinical attenuation in cattle but does not prevent subclinical infection. Virology 516:115–126. https://doi.org/10.1016/j.virol.2018.01.008.
41. Fish I, Stenfeldt C, Palinski RM, Pauszek SJ, Arzt J. 2020. Into the deep (sequence) of the foot-and-mouth disease virus gene pool: bottlenecks and adaptation during infection in naive and vaccinated cattle. Pathogens 9:208. https://doi.org/10.3390/pathogens9030208.
42. Dekker A, Vernooij H, Bouma A, Stegeman A, Tenzin. 2008. Rate of foot-and-mouth disease virus transmission by carriers quantified from experimental data. Risk Anal 28:303–309. https://doi.org/10.1111/j.1539-6924.2008.01020.x.
43. Pacheco JM, Stenfeldt C, Rodriguez LL, Arzt J. 2016. Infection dynamics of foot-and-mouth disease virus in cattle following intranasopharyngeal inoculation or contact exposure. J Comp Pathol 155:314–325. https://doi.org/10.1016/j.jcpa.2016.08.005.
44. Brown F, Cartwright B. 1960. Purification of the virus of foot-and-mouth disease by fluorocarbon treatment and its dissociation from neutralizing antibody. J Immunology 85:309–313. https://doi.org/10.4049/jimmunol.85.3.309.
45. Callahan JD, Brown F, Osorio FA, Sur JH, Kramer E, Long GW, Lubroth J, Ellis SJ, Shoulars KS, Gaffney KL, Rock DL, Nelson WM. 2002. Use of a portable real-time reverse transcriptase-polymerase chain reaction assay for rapid detection of foot-and-mouth disease virus. J Am Vet Med Assoc 220:1636–1642. https://doi.org/10.2460/javma.2002.220.1636.
46. Rasmussen TB, Uttenthal A, de Stricker K, Belak S, Storgaard T. 2003. Development of a novel quantitative real-time RT-PCR assay for the simultaneous detection of all serotypes of foot-and-mouth disease virus. Arch Virol 148:2005–2021. https://doi.org/10.1007/s00705-003-0145-2.
47. Stenfeldt C, Pacheco JM, Smoliga G, Bishop E, Pauszek S, Hartwig E, Rodriguez L, Arzt J. 2016. Detection of foot-and-mouth disease virus RNA and capsid protein in lymphoid tissues of convalescent pigs does not indicate existence of a carrier state. Transbound Emerg Dis 63:152–164. https://doi.org/10.1111/tbed.12235.
48. LaRocco M, Krug PW, Kramer E, Ahmed Z, Pacheco JM, Duque H, Baxt B, Rodriguez LL. 2013. A continuous bovine kidney cell line constitutively expressing bovine $\alpha v\beta 6$ integrin has increased susceptibility to foot-and-mouth disease virus. J Clin Microbiol 51:1714–1720. https://doi.org/10.1128/JCM.03370-12.
49. Swaney LM. 1988. A continuous bovine kidney cell line for routine assays of foot-and-mouth disease virus. Vet Microbiol 18:1–14. https://doi.org/10.1016/0378-1135(88)90111-3.
50. Pacheco JM, Arzt J, Rodriguez LL. 2010. Early events in the pathogenesis of foot-and-mouth disease in cattle after controlled aerosol exposure. Vet J 183:46–53. https://doi.org/10.1016/j.tvjl.2008.08.023.
51. LaRocco M, Krug PW, Kramer E, Ahmed Z, Pacheco JM, Duque H, Baxt B, Rodriguez LL. 2015. Correction for LaRocco et al., a continuous bovine kidney cell line constitutively expressing bovine $\alpha V\beta 6$ integrin has increased susceptibility to foot-and-mouth disease virus. J Clin Microbiol 53:755. https://doi.org/10.1128/JCM.03220-14.
52. Arzt J, Gregg DA, Clavijo A, Rodriguez LL. 2009. Optimization of immunohistochemical and fluorescent antibody techniques for localization of foot-and-mouth disease virus in animal tissues. J Vet Diagn Invest 21:779–792. https://doi.org/10.1177/104063870902100604.